

# Sepage below Horizontal Apron with Downstream Cutoff, Founded on Anisotropic Pervious Medium of Finite Depth

by

Alam Singh\*

B.C. Punmia\*\*

## Introduction

IF a hydraulic structure is built upon pervious soil, and water-level upstream of the structure is higher than it is downstream, percolation will occur in the underlying permeable soil. The percolation may cause undermining of the pervious granular structure which would necessarily be followed by the collapse of the whole structure. In addition to this, the floor or the apron may be forced upward, owing to the upward pressure of water seeping through the pervious soil under the structure.

Clibborn and Beresford (1895-97) enunciated the 'hydraulic gradient theory of weir design' which formed the basis of the Bligh's creep theory (1910). A general theory, and a large number of individual solutions of the conformal transformation problems as applied to weir foundation design were published by Prof. N.N. Pavlovsky (1922, 1933). Weaver (1932) analysed mathematically the problem of uplift pressure on the base, for the case of a dam on homogeneous sand of infinite depth, with the base of the dam resting on, and level with, the sand surface, with and without a single line of sheet piling. These solutions provided the inspiration for more generalised theoretical solutions by Khosla, Bose and Taylor (1936). The charts given by them still form the basis of scientific design of weir aprons in India.

Khosla and his associates made two very important assumptions in their solutions : (i) the soil medium is of infinite depth and (ii) the soil medium is isotropic. The porous medium may be anisotropic and of finite depth. The purpose of the present investigation is to take into account all these factors, not accounted for in the Khosla theory, and prepare the design curves to find the uplift pressure at any point below the weir floor having a pile at its downstream end. The problem has been investigated experimentally by electrical analogy, and the results have been verified by the theoretical solution, based on the original solution given by Pavlovsky, taking into account the anisotropy of the soil medium. The theoretical solution has been given in brief in Appendix I.

---

\* Professor and Head of Civil Engineering Department, University of Jodhpur, Jodhpur.

\*\* Reader in Civil Engineering, University of Jodhpur, Jodhpur.

*This paper was received on 3 December 1971. It is open for discussion up to December 1973.*

### Experimental Set-up

In the present investigation, an electrical analogy tray of size  $1.2 \text{ m} \times 1.5 \text{ m} \times 6.4 \text{ cm}$  was used. The bottom of the tray was made of a  $6.4 \text{ mm}$  thick glass plate placed on a graph paper marked with reference axes and co-ordinates. The transparency of the glass sheet enabled in reading the co-ordinates of any desired point of the foundation. The sides of the tank were made of  $3.2 \text{ mm}$  thick and  $6.4 \text{ cm}$  high perspex strips pasted to  $2.5 \text{ cm}$  thick and  $6.4 \text{ cm}$  high timber strips with fevicol solution. The tray was fixed to a rigid frame work of wood at its bottom to prevent the deflection of its bottom. Figure 1 shows diagrammatically the tray with the model and the circuit diagram. A step-down transformer was used to supply a  $20 \text{ V} = 50$  cycles current. Two decade-resistance boxes were connected in parallel with the alternating current. These resistance boxes worked as a potential divider. A.D.C. galvanometer of sensitivity  $50.0\text{-}50 \mu\text{A}$  was used for null-point indication, and the current was supplied to it through a diode. Figure 2 shows the photographs of the complete set-up.

### Model Dimensions

Figure 3 illustrates the problem under investigation. The principal model parameters are: (i) the base width of the apron,  $b$ , (ii) the depth of

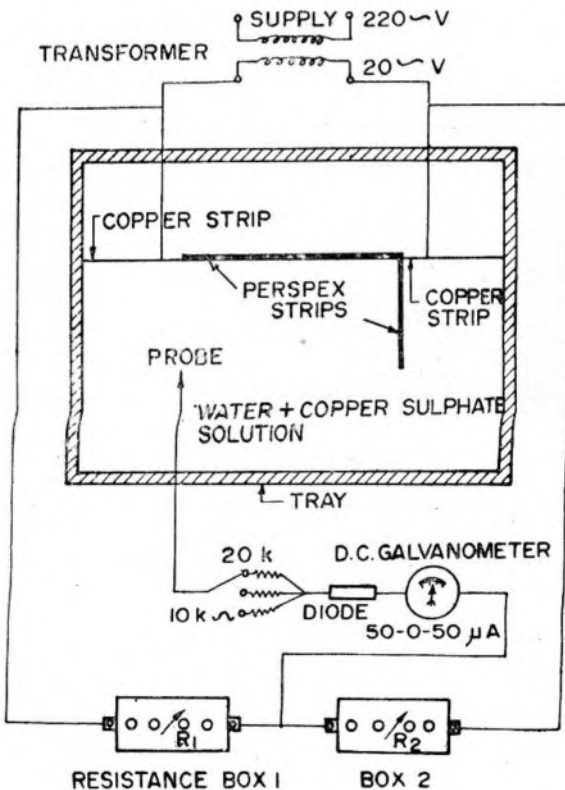


FIGURE 1: The Circuit diagram.

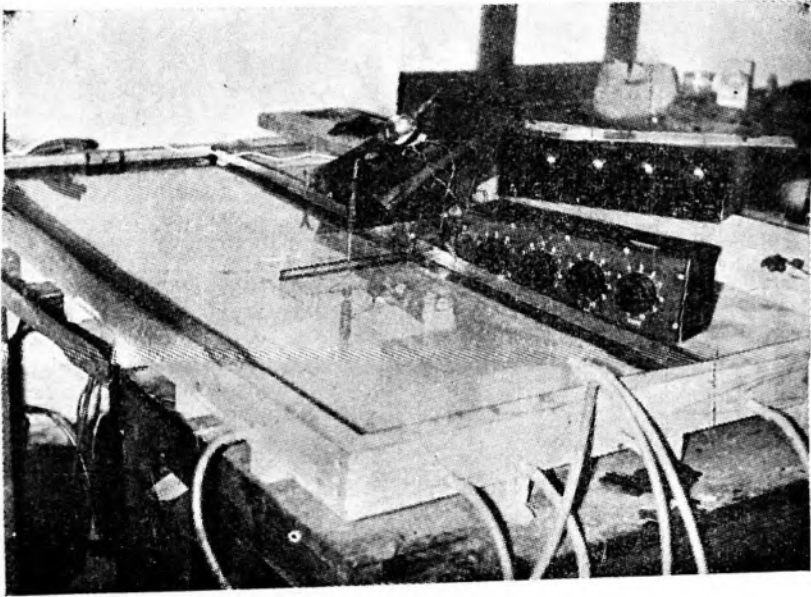


FIGURE 2 : Model set-up.

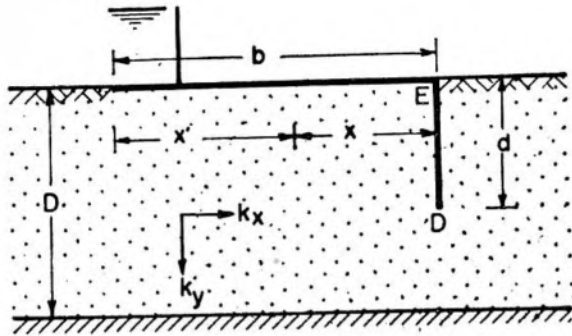


FIGURE 3 : The problem.

the downstream pile,  $d$ , (iii) the finite depth of the pervious medium,  $D$  and (iv) the anisotropy ratio  $n = k_x/k_y$  where  $k_x$  and  $k_y$  are the coefficients of permeability in the  $x$  and  $y$  directions respectively. In all, 80 models were tested, by suitably varying the above parameters (Punmia, 1969).

The tests were divided into four series : (A) : Isotropic soil, (B) anisotropic soil,  $k_x = 4 k_y$ , (C) anisotropic soil,  $k_x = 9 k_y$  and (D) anisotropic soil,  $k_x = 16 k_y$ . In each series, twenty models (i.e.,  $A_1, A_2, \dots, A_{20}$ ) were tested, to represent various  $b/D$ ,  $b/d$  and  $d/D$  ratios.  $b/D$  ratio was kept as  $\frac{1}{4}$ ,  $\frac{1}{2}$ ,  $\frac{3}{4}$ , 1 and 2.  $d/D$  ratio (i.e., penetration ratio  $p$ ) was kept as 0.2, 0.4, 0.6, and 0.8 to see the effect of percentage penetration of the downstream pile on the uplift pressure.  $b/d$  ratio was varied from 0.3125 to 10. In the case of anisotropic soil, the model dimensions were made to natural

scale in the  $y$ -direction while all dimensions parallel to  $x$ -axis were reduced by multiplying by the factor  $\sqrt{k_y/k_x}$ .

### Observations

The potential at any point below the floor was measured by suitably selecting the values of  $R_1$  and  $R_2$  of the resistances of the two decade resistance boxes so that null is obtained. Each resistance box contains 4 knobs. The first knob has resistance variations from 0 to 10 ohms in the steps of 1 ohm. The second knob has resistance variation from 0 to 100 ohms in the steps of 10 ohms. The third knob has resistance variations from 0 to 1000 ohms in the steps of 100 ohms. Lastly, the fourth knob has resistance variations from 0 to 10000 ohms in the steps of 1000 ohms. Since both the boxes are connected in series, the total resistance  $R$  is given by

$$R = R_1 + R_2$$

Hence the percent potential  $\phi$  at the point of measurement is given by

$$\phi = \frac{R_2}{R_1 + R_2} \times 100$$

For convenience in calculations, the resistance  $R_2$  was set up at 10 or 100 ohms and the resistance  $R_1$  was then varied by suitably moving the appropriate knobs, till null point was indicated. For null point indication current was fed to the galvanometer through 'coarse' and 'medium' settings and finally through the 'fine setting' to get the null point accurately, and to safeguard the galvanometer against heavy deflections in the initial settings of  $R_1$ .

### Analysis of Results

The analysis of test results, along with the computed values with the help of theoretical expressions (Appendix-I) have been divided into two heads :—

(a) Influence of  $b/D$ ,  $b/d$ ,  $n (=k_x/k_y)$  and  $p (=d/D)$  on pressure distribution ( $\phi_x$ ) :

(i) Variation of  $\phi_x$  with  $x'/b$ ,  $p$  and  $b/d$ , for fixed values of  $b/D$  ratio.

(ii) Variation of  $\phi_x$  with  $x'/d$ ,  $p$  and  $b/D$  ratio, for fixed values of  $b/d$  ratio.

(iii) Variation of  $\phi_x$  with  $x'/b$ ,  $p$  and  $b/D$  ratio for fixed values of  $b/d$  ratio.

(iv) Variation of  $\phi_x$  with  $x'/b$ ,  $b/D$  and  $b/d$ , for fixed values of  $p$ .

(v) Effect of anisotropy ratio  $n$  on  $\phi_x$ .

(b) Influence of  $b/D$ ,  $n$  and  $p$  on  $\phi_E$  and  $\phi_D$

(vi) Influence of  $D/b$  ratio on  $\phi_E$  and  $\phi_D$  for a given value of percent penetration of pile.

- (vii) Influence of percent penetration of pile on  $\phi_E$  and  $\phi_D$  with  $b/d$  ratios.
- (viii) Variation of  $\phi_E$  and  $\phi_D$  with  $b/d$  ratio and anisotropy for fixed values of  $b/D$  ratios.

#### INFLUENCE of $b/D$ , $b/d$ , $n$ AND $p$ ON PRESSURE DISTRIBUTION

Figure 4 shows the variation of  $\phi_x$  for a typical case of  $b/D = \frac{1}{2}$  (fixed), isotropic condition and the values of  $p$  and  $b/d$  for the four curves as follows:  $p=0.2$  and  $b/d=2.5$  for the first curve;  $p=0.4$  and  $b/d=1.25$  for the second curve;  $p=0.6$  and  $b/d=5/6$  for the third curve and  $p=0.8$  and  $b/d=5/8$  for the fourth curve. Khosla's curve for  $b/d=2.5$ , assuming infinite depth of pervious medium is shown dotted, for comparison. The Khosla curve for  $\phi_x$  has been computed from the following expression :

$$\phi_x = \frac{1}{\pi} \frac{\cos^{-1} \lambda_1 - \sqrt{1 + (x_1/d)^2}}{\lambda} ; \quad \frac{b}{d} = \alpha = 2.5$$

where, 
$$\lambda = \frac{\sqrt{1 + \alpha^2} + 1}{2} = \frac{\sqrt{1 + (2.5)^2} + 1}{2} = 1.845$$

$$\lambda_1 = \frac{\sqrt{1 + \alpha^2} - 1}{2} = \frac{\sqrt{1 + (2.5)^2} - 1}{2} = 0.845$$

$x_1$  = horizontal distance of any point under the floor, measured from the pile line.

Figure 5 shows the variation of  $\phi_x$  for the case when  $b/D = 1$ . The four curves correspond to the values of  $p$  as 0.2, 0.4, 0.6 and 0.8. Similarly, Figure 6 shows the pressure distribution when  $b/D = 2$ .

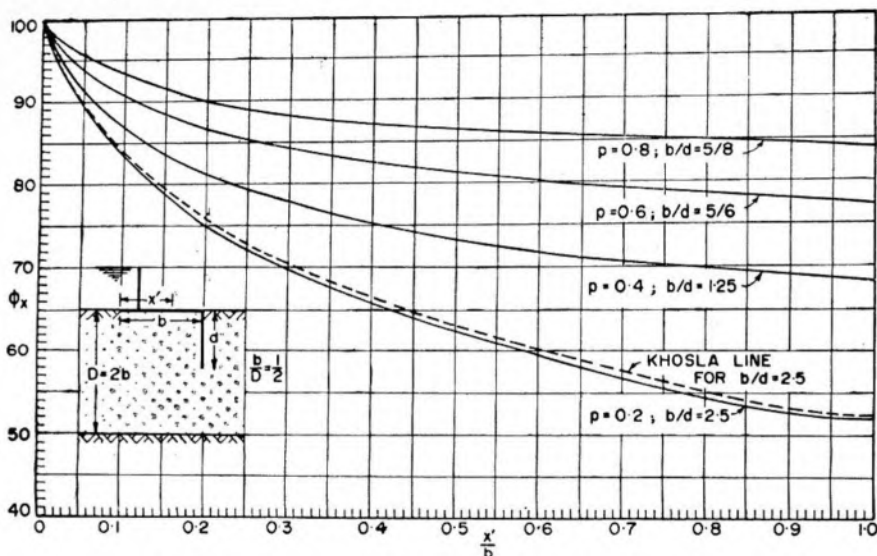


FIGURE 4: Variation of  $\phi_x$  for various values of  $p$  and  $b/d$ .  
 $b/D = \frac{1}{2}$  (Fixed); Isotropic case.

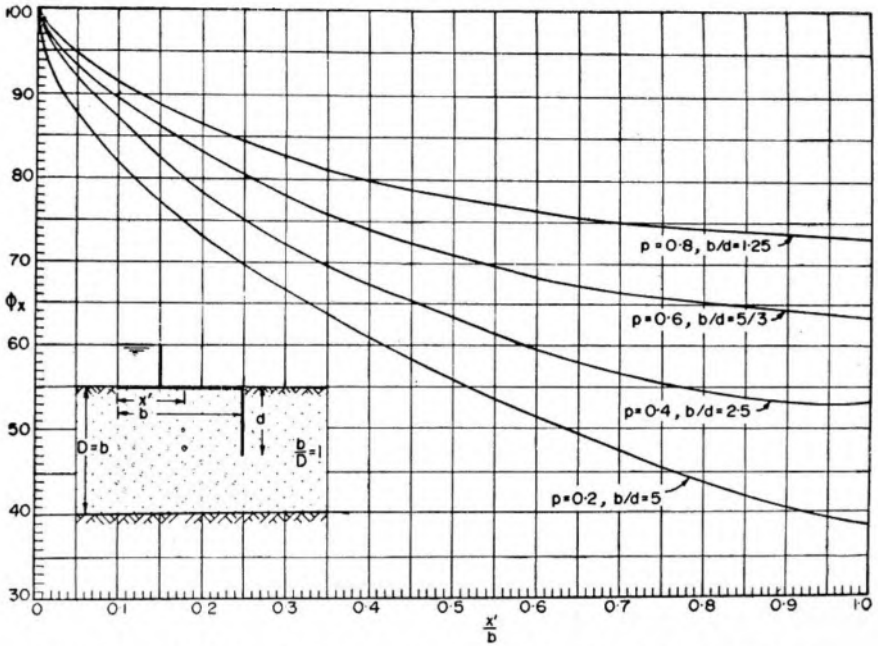


FIGURE 5: Variation of  $\phi_x$  for various values of  $p$  and  $b/d$ .  $b/D=1$  (Fixed); Isotropic case.

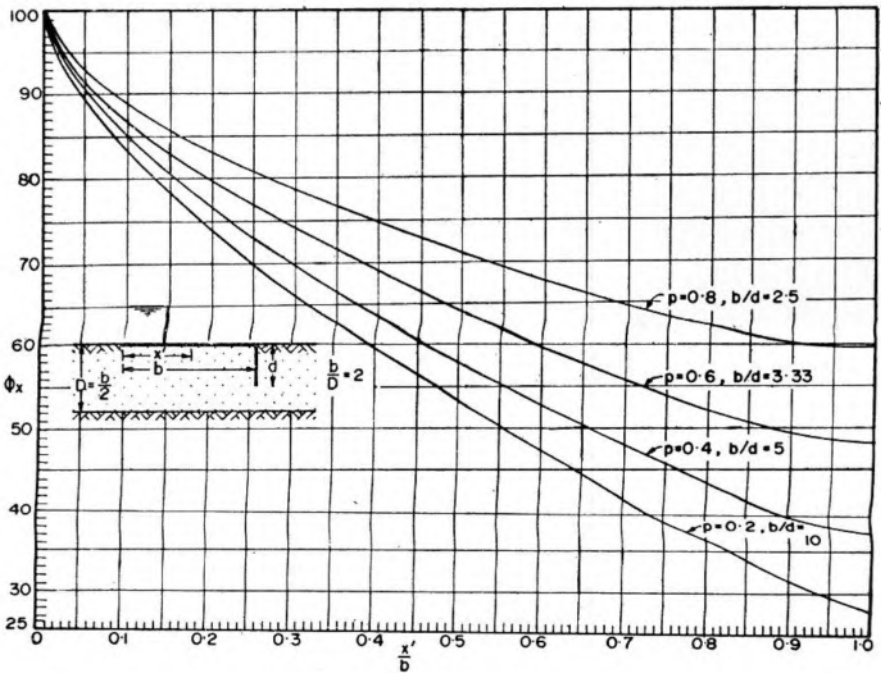


FIGURE 6: Variation of  $\phi_x$  for various values of  $p$  and  $b/d$ .  $b/D=2$  (Fixed); Isotropic case.

Figure 7 shows the variation of  $\phi_x$  with  $x'/b$  ratio, for a typical case of  $b/d=2.5$  (fixed). The values of  $p$  are 0.2, 0.4 and 0.8 and those of  $b/D$  are  $\frac{1}{2}$ , 1 and 2 respectively for the three curves. Khosla's line of  $\phi_x$  for  $b/d=2.5$  has been shown for comparison.

In order to study the effect of anisotropy on the pressure distribution under the apron, various values of  $p$ ,  $b/d$  and  $b/D$  were chosen. Figure 8 shows a typical set of curves of variations of  $\phi_x$  with  $x'/b$  and anisotropy ratio  $n$ , for the following fixed values;  $p=0.4$ ;  $b/D=2$  and  $b/d=5$ . The Khosla line for  $\phi_x$  when  $b/d=5$  is shown by a dotted curve.

#### INFLUENCE OF $b/D$ , $b/d$ , $n$ AND $p$ ON $\phi_E$ AND $\phi_D$

The pressures at the key points  $E$  and  $D$  depend upon  $b/d$ ,  $b/D$ ,  $p$  and  $n$ . In order to see the influence of  $D/b$  ratio on  $\phi_E$  and  $\phi_D$  two values of  $p$  were selected:  $p=0.2$  and  $p=0.4$ .  $D/b$  ratio was varied from  $\frac{1}{2}$  to 4. Figure 9(a) shows the variation of  $\phi_E$  for  $p=0.2$ , while Figure 9(b) shows the variation of  $\phi_D$  for  $p=0.2$ . Similarly, Figure 10(a) and (b) respectively shows the variations of  $\phi_E$  and  $\phi_D$  when  $p=0.4$ . In each of these diagrams, the values of  $n (=k_x/k_y)$  were 1, 4, 9 and 16.

Figure 11 (a) and (b) shows respectively the variations of  $\phi_E$  and  $\phi_D$  with the pile penetration  $p$  and anisotropy ratio  $n$ , for the typical case when  $b/D=1$ . Similarly, Figure 12(a) and (b) shows respectively the variations of  $\phi_E$  and  $\phi_D$  with  $p$  and  $n$ , when  $b/D=2$ .

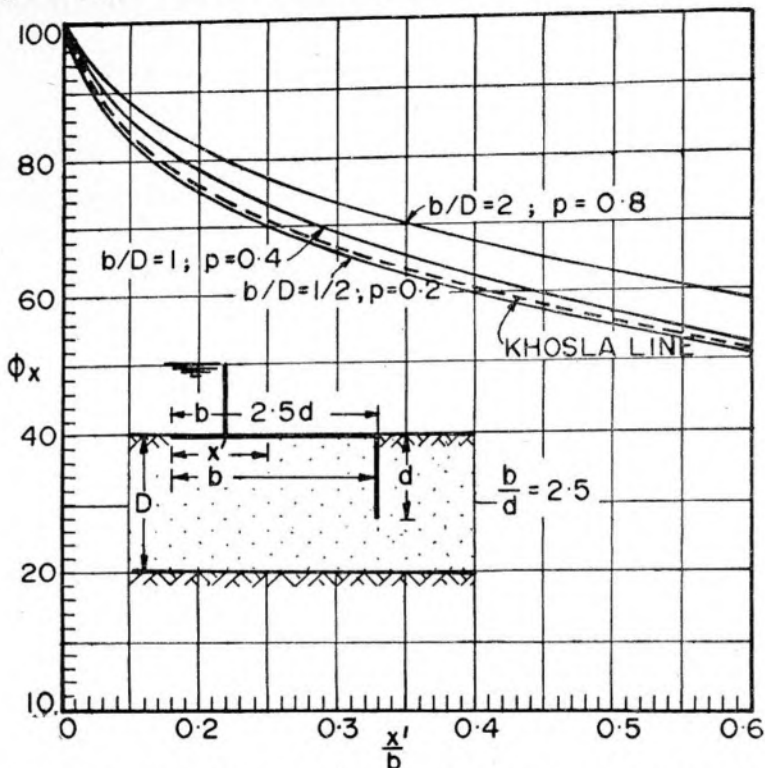


FIGURE 7: Variation of  $\phi_x$  for various values of  $p$  and  $b/d$ .  $b/D=2.5$  (Fixed); Isotropic case.



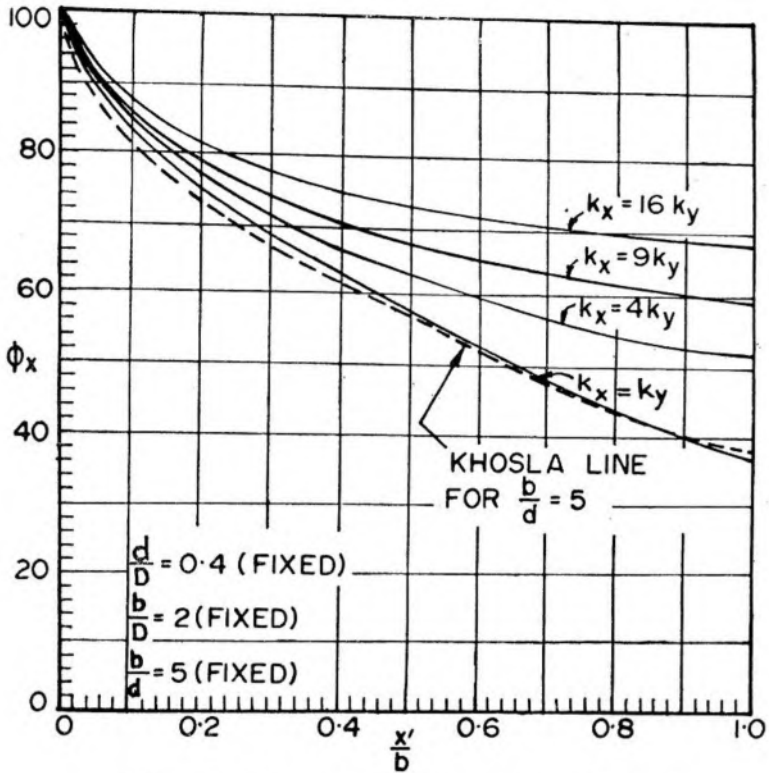


FIGURE 8 : Effect of anisotropy on pressure distribution.

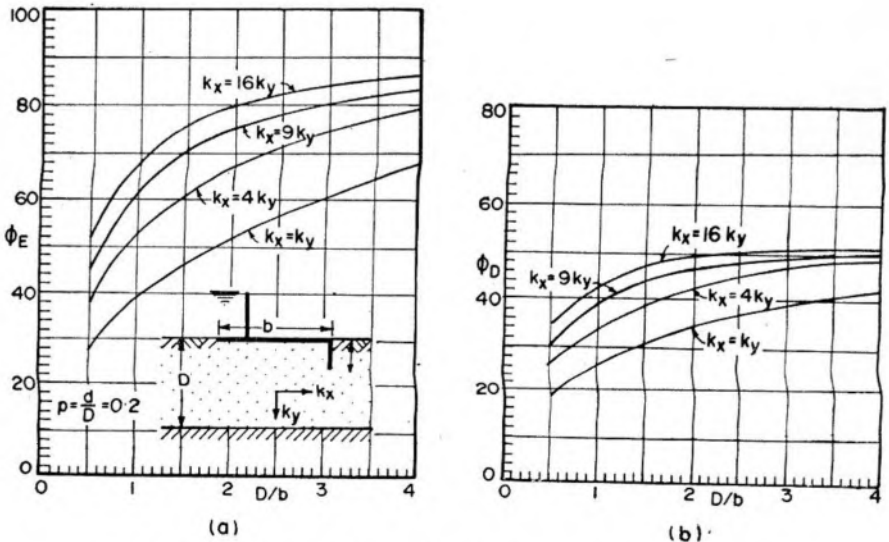


FIGURE 9 (a & b) : Influence of  $D/b$  ratio on  $\phi_E$  and  $\phi_D$  ( $p=0.2$ ).



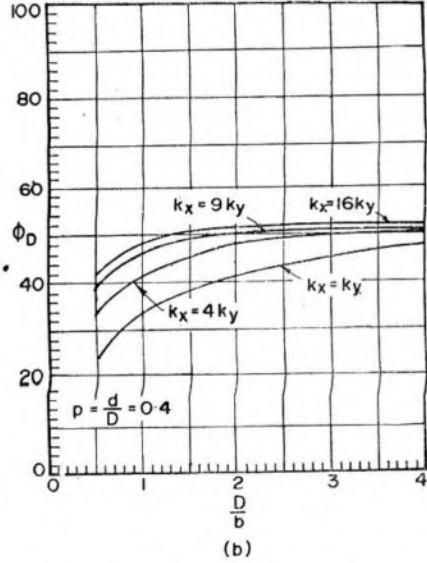
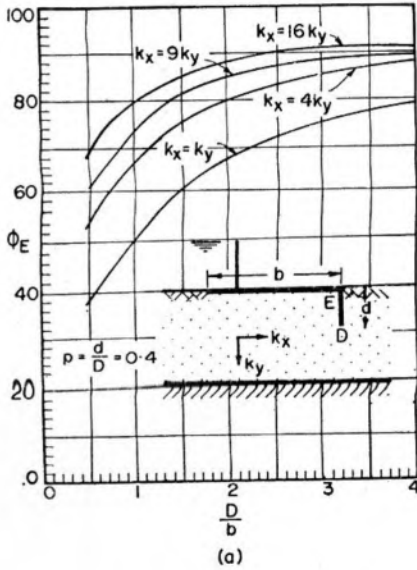


FIGURE 10 (a & b) : Influence of  $D/b$  ratio on  $\phi_E$  and  $\phi_D$  ( $p=0.4$ ).

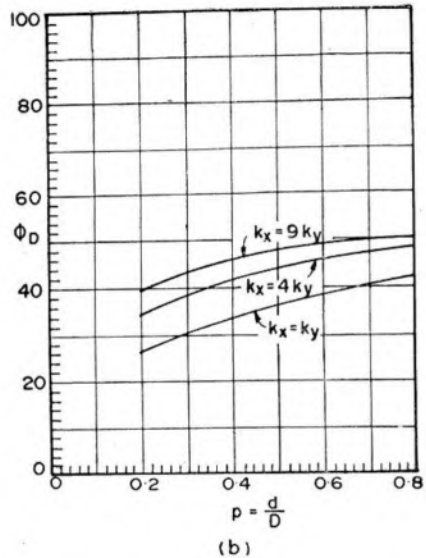
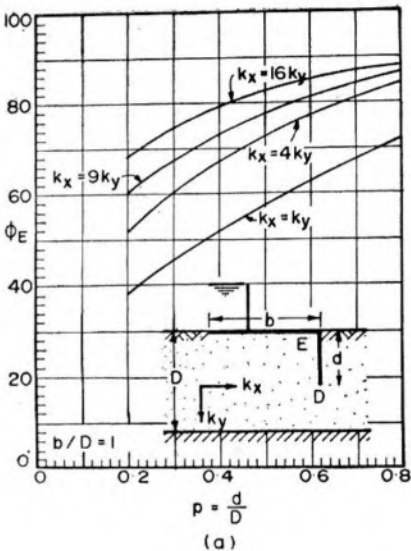


FIGURE 11 (a & b) : Influence of  $p$  on  $\phi_E$  and  $\phi_D$  ( $b/D=1$ ).

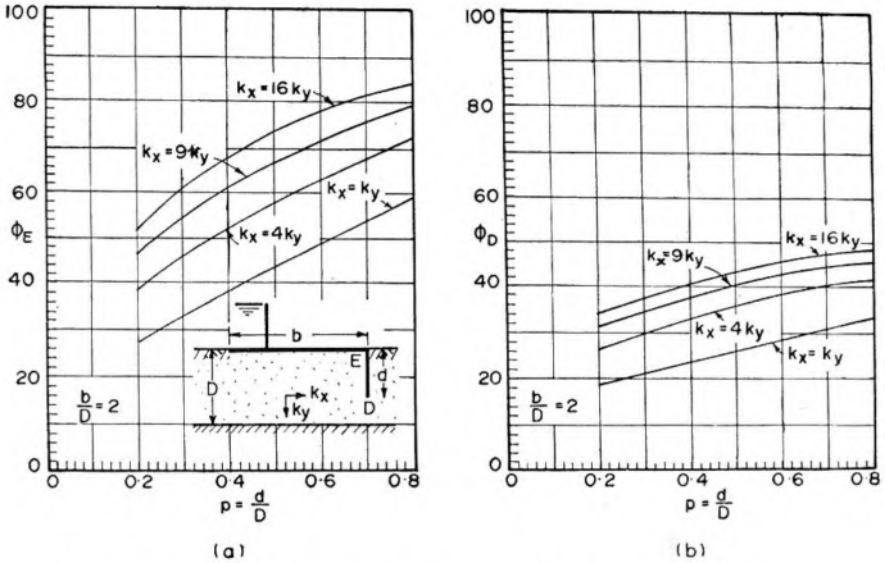


FIGURE (a & b) 12 : Influence of  $p$  on  $\phi_E$  and  $\phi_D$  ( $b/D=2$ ).

### DESIGN CURVES

From design point of view, it is essential to have design curves for  $\phi_E$  and  $\phi_D$ , showing variations of these with  $b/d$  ratio, for all the four anisotropy ratios, and a series of  $b/D$  ratio. Khosla and his associates have given design curves for  $\phi_E$  and  $\phi_D$  assuming infinite depth (i.e.,  $b/D=0$ ) and treating the soil to be isotropic. In the present case,  $b/D$  ratio is finite and anisotropy of the soil has been taken into consideration.

Figure 13 gives the design curves for  $\phi_E$  for  $b/D=2$  (fixed), the variation being plotted against the  $b/d$  ratios. All the four cases of  $k_x/k_y$  ratios give rise to four curves for  $\phi_E$ . On the same figure, Khosla curve for  $\phi_E$  has also been drawn. The minimum value of  $b/d$  ratio (when  $b/D=2$ ) will be 2 when  $p$  is 100 percent. Figure 14 gives the design curves for  $\phi_D$  for all the four anisotropy ratios. Similarly, Figure 15(a) and (b) respectively shows the design curves for  $\phi_E$  and  $\phi_D$  when  $b/D=1$ .

### COMPARISON WITH THE THEORETICAL RESULTS

The theoretical solution of the present case has been given in Appendix I. The solution is based on the lines of the original solution given by Pavlovsky (1923). However, the present solution has been slightly modified, taking into account the anisotropy of the soil medium. It has been found that the experimental values are in close agreement with the computed values, the error being within 2 percent.

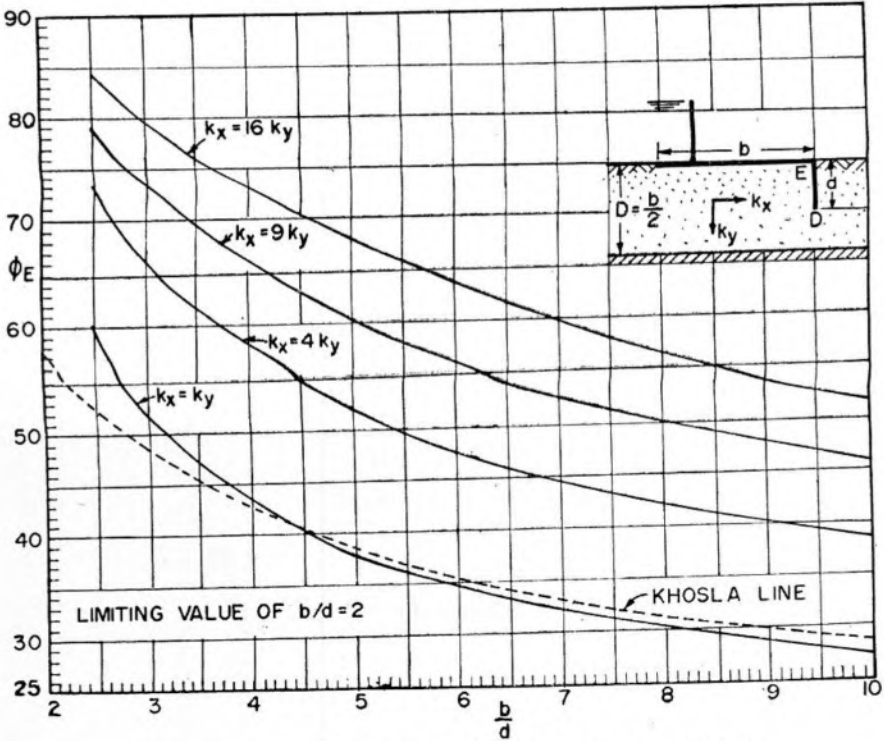


FIGURE 13 : Variation of  $\phi_E$  with  $b/d$  and anisotropy ( $b/D=2$ ).

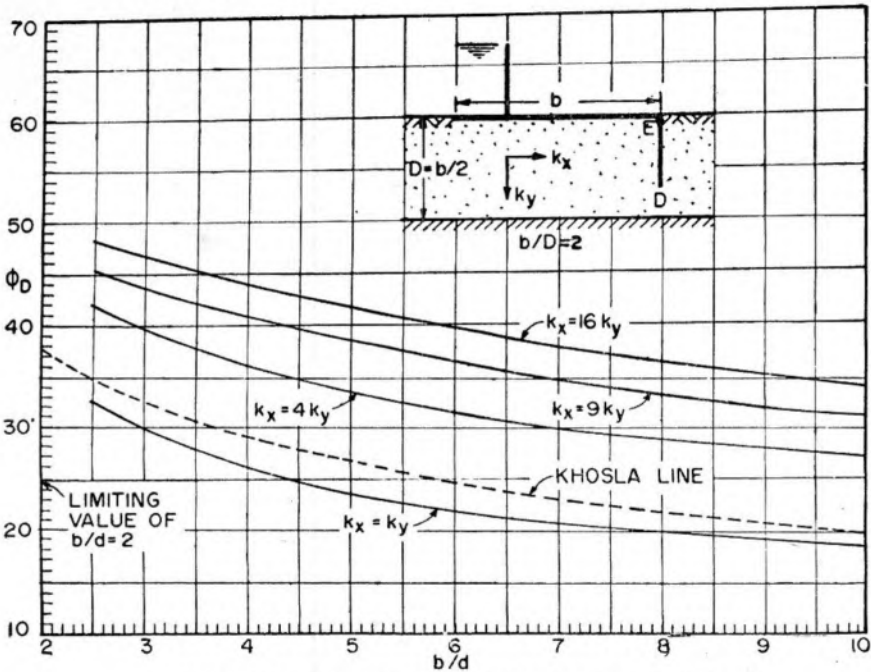


FIGURE 14 : Variation of  $\phi_D$  with  $b/d$  and anisotropy ( $b/D=2$ ).

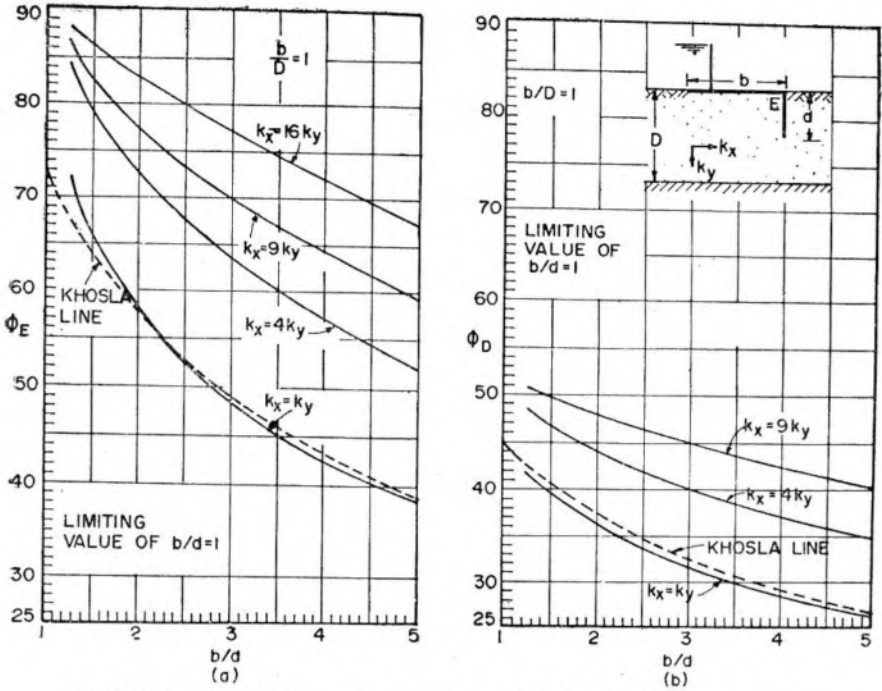


FIGURE 15 : Variation of  $\phi_E$  and  $\phi_D$  with  $b/d$  and anisotropy ( $b/D=1$ ).

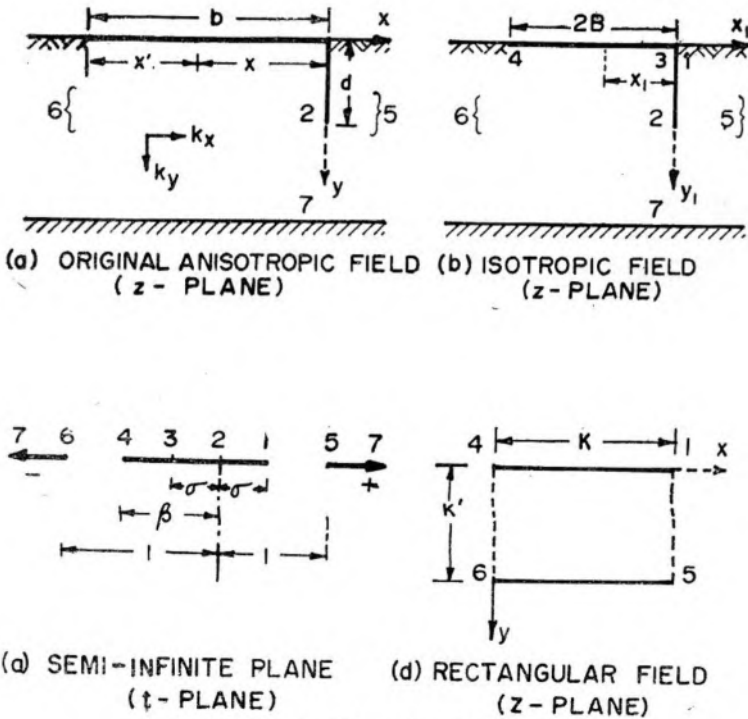


FIGURE 16 : Theoretical solution.

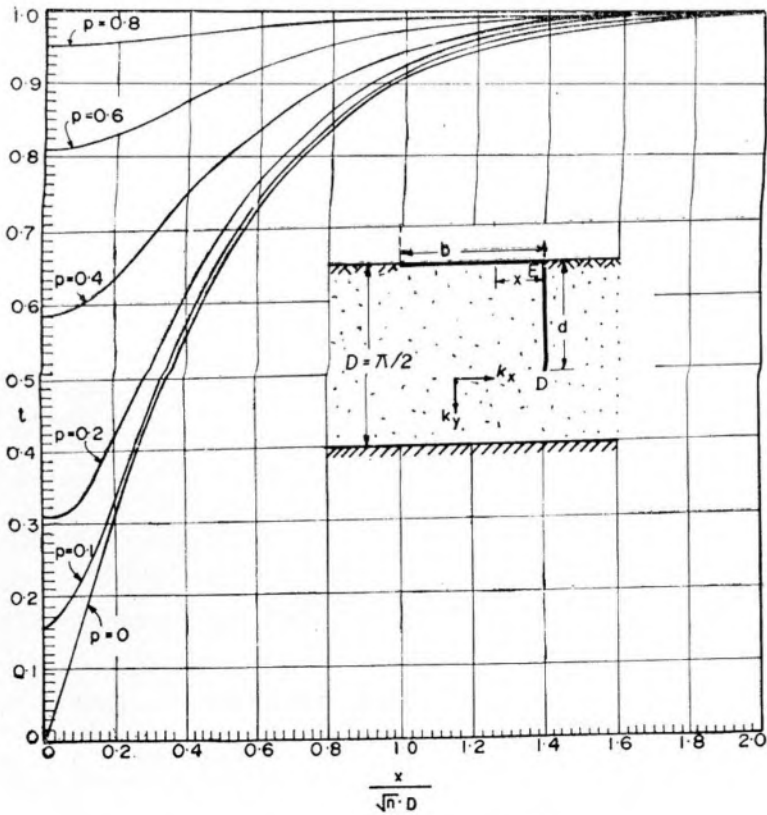


FIGURE 17 : Variation of  $t$  with  $p$  and  $\frac{x}{\sqrt{n} \cdot D}$ .

### Conclusions

From the test observations on the electrical analogy models as well as from the theoretical computations, the following conclusions are drawn :

- (1) For a given  $b/D$  ratio, the pressure at any point increases as the percent penetration of the pile increases. However, the variation of this pressure with  $x'/b$  is larger for lower values of  $p$ .
- (2) For a given  $b/D$  ratio, pressure at any point decreases as  $b/d$  ratio increases.
- (3) For isotropic soil, the effect of infinite depth comes when  $b/D \leq \frac{1}{2}$  (or  $D/b \geq 2$ ) approximately. However, for anisotropic case, the effect of infinite depth comes when  $\frac{b}{D} \leq \frac{1}{2\sqrt{n}}$  (or  $\frac{D}{b} \geq 2\sqrt{n}$ ).
- (4) For very small penetration ratios, the pressure distribution can be found even by assuming infinite depth (i.e., by using Khosla's theory).

- (5) The pressure at any point increases sharply with increase in anisotropy.
- (6) The pressure variation under the floor is of smaller magnitude for a greater anisotropy ratios.
- (7) For a given value of penetration ratio  $p$ ,  $\phi_E$  and  $\phi_D$  increase as  $D/b$  increases.
- (8) For a given  $D/b$  ratio and  $p$ ,  $\phi_E$  and  $\phi_D$  increase with increase in the anisotropy. Hence the usual assumption of isotropic medium should be made with caution, as it may lead to unsafe designs.
- (9) The effect of anisotropy is more pronounced at lower values of  $D/b$  (i.e., for finite depth case).
- (10)  $\phi_E$  and  $\phi_D$  decrease with increasing values of  $b/d$  ratio.

## APPENDIX I

### Theoretical Solution

The theoretical solution given herein is based on theoretical solutions by Pavlovsky (1922), taking into account the effect of anisotropy of the soil medium. Figure 16(a) shows the problem under consideration. The solution is obtained by performing three operations : (1) transformation of  $z$ -plane [Figure 16 (a)] of original anisotropic medium into  $z$ -plane [Figure 16 (b)] of isotropic medium, (2) transformation of  $z$ -plane [Figure 16 (b)] of isotropic medium into semi-infinite  $t$ -plane [Figure 16 (c)] and (3) transformation of  $z$ -plane of rectangular field [Figure 16 (d)] into the semi-infinite  $t$ -plane [Figure 16 (c).]

#### FIRST OPERATION

The given anisotropic plane is transformed into isotropic plane by the following equations :

$$x_1 = x\sqrt{k_y/k_x} = \frac{x}{\sqrt{n}} \quad \dots(1a)$$

and  $y_1 = y$

Thus,  $B = \frac{b}{2\sqrt{n}}$

where  $n = k_x/k_y = \text{anisotropy ratio}$

#### SECOND OPERATION

To transform the isotropic  $z$ -plane into semi-infinite  $t$ -plane, the corresponding points in the two planes are chosen as follows :

$$\begin{aligned} z_2 = id & \quad ; \quad t_2 = 0 \\ z_5 = +\infty & \quad ; \quad t_5 = +1 \\ z_6 = -\infty & \quad ; \quad t_6 = -1 \end{aligned}$$

also, due to symmetry of general layout

$$t_1 = t_3 = \sigma \text{ (say)}$$

The Schwarz-Christoffel transformation formula for the present case is

$$z = A \int \frac{dt}{(t_1-t)^{\lambda_1} (t_2-t)^{\lambda_2} (t_3-t)^{\lambda_3} (t_5-t)^{\lambda_5} (t_6-t)^{\lambda_6}} + N \quad \dots(2)$$

which reduces to

$$z = A \int \frac{t \cdot dt}{(1-t^2) \sqrt{\sigma^2 - t^2}} + N \quad \dots(3)$$

Integrating the above expression between five specific intervals of  $t$  (i.e.,  $-\infty < t < -1$ ;  $-1 < t < -\sigma$ ;  $-\sigma < t < +\sigma$ ;  $+\sigma < t < 1$  and  $1 < t < \infty$ ), substituting the values of co-ordinates of points 1, 2 and 7, and choosing the 'main dimension'  $D = \pi/2$  the above integral reduces to one single expression :

$$z = \pm \tanh^{-1} \frac{\sqrt{t^2 - \sigma^2}}{\sigma_1} \quad \dots(4)$$

where  $\sigma = \sin\left(\frac{\pi}{2} \cdot \frac{d}{D}\right) = \sin d$

$$\sigma_1 = \sqrt{1 - \sigma^2} = \cos d$$

substituting the values of  $\sigma$  and  $\sigma_1$  in (4), the required transformation equation becomes

$$t = \pm \cos d \sqrt{\tanh^2 z + \tanh^2 d} \quad \dots(5)$$

For all points under the floor, the value of  $t$  is given by

$$\begin{aligned} t &= \cos d \sqrt{\tanh^2 x_1 + \tanh^2 d} \\ &= \cos \frac{\pi}{2} \cdot \frac{d}{D} \sqrt{\tanh^2 \frac{\pi}{2} \cdot \frac{x_1}{D} + \tanh^2 \frac{\pi}{2} \cdot \frac{d}{D}} \end{aligned} \quad \dots(6a)$$

$$= \cos \frac{\pi}{2} p \sqrt{\tanh^2 \frac{\pi}{2} \cdot \frac{x}{\sqrt{n} \cdot D} + \tanh^2 \frac{\pi}{2} \cdot p} \quad \dots(6)$$

Table I and Figure 17 give the values of  $t$  for various values of  $p$  ( $= \frac{d}{D}$ ) and  $\frac{x}{\sqrt{n} \cdot D}$  ratio. Again, from Equation (5),

$$\beta = t_4 = \cos d \sqrt{\tanh^2 2B + \tanh^2 d} \quad \dots(7a)$$

$$= \cos d \sqrt{\tanh^2 \frac{b}{\sqrt{n}} + \tanh^2 d} \quad \dots(7b)$$

$$= \cos \frac{\pi}{2} p \sqrt{\tanh^2 \frac{\pi}{2} \cdot \frac{b}{\sqrt{n} \cdot D} + \tanh^2 \frac{\pi}{2} \cdot p} \quad \dots(7)$$

$\beta$  can be determined from Table I or Figure 17



TABLE I

$$t = \cos \frac{p\pi}{2} \sqrt{\tanh^2 \frac{\pi}{2} \frac{x}{\sqrt{n.D}} + \tan^2 \frac{p\pi}{2}}$$

$\frac{x}{\sqrt{n.D}}$	$p=0.2$	0.4	0.6	0.8
0.0	0.309017	0.587784	0.809022	0.951064
0.1	0.342742	0.601162	0.814059	0.952285
0.2	0.423311	0.637227	0.828619	0.955399
0.3	0.519591	0.686847	0.849280	0.960699
0.4	0.613232	0.740645	0.872768	0.966511
0.5	0.696060	0.791886	0.896168	0.972408
0.6	0.765476	0.836860	0.917540	0.977909
0.7	0.821391	0.874483	0.935854	0.982664
0.8	0.865555	0.904709	0.950909	0.986689
0.9	0.899508	0.923380	0.962845	0.989875
1.0	0.925382	0.946607	0.978053	0.992397
1.1	0.944847	0.960393	0.979303	0.994321
1.2	0.959331	0.970740	0.985153	0.995795
1.3	0.969412	0.977967	0.988443	0.996825
1.4	0.979379	0.984164	0.991614	0.9977105
1.5	0.983940	0.988339	0.993858	0.998310
1.6	0.988215	0.991486	0.995528	0.998762
1.7	0.991362	0.993724	0.996684	0.999092
1.8	0.993673	0.995422	0.997594	0.999352
2.0	0.996622	0.997562	0.998731	0.999658
2.5	0.999284	0.999476	0.999735	0.9999668
3.0	0.999845	0.999886	0.999923	0.9999936
3.5	0.999969	0.999977	0.999997	0.9999976
4.0	1.000000	0.999992	1.000000	0.9999995

## THIRD OPERATION

The Schwarz-Christoffel transformation formula is

$$dZ = \frac{A \cdot dt}{(t-t_4)(t-t_1)(t-t_5)(t-t_6)}$$

This, on integration, reduces to

$$t = \frac{t_4(t_6-t_1) - t_7(t_4-t_1) \operatorname{Sn}^2 \frac{MZ}{A}}{(t_6-t_1) - (t_4-t_1) \operatorname{Sn}^2 \frac{MZ}{A}} \quad \dots(8)$$

Choosing  $A=M$

$$t = \frac{t_4(t_6-t_1) - t_6(t_4-t_1) \operatorname{Sn}^2 Z}{(t_6-t_1) - (t_4-t_1) \operatorname{Sn}^2 Z} \quad \dots(9)$$

$$\text{or } Z = \operatorname{Sn}^{-1} \left( \sqrt{\frac{(t_6-t_1)(t_4-t)}{(t_4-t_1)(t_6-t)}}, m \right) \quad \dots(10a)$$

$$= \operatorname{Sn}^{-1} \left( \sqrt{\frac{(1+\sigma)(\beta-t)}{(\beta+\sigma)(1-t)}}, m \right) \quad \dots(10)$$

$$= \operatorname{Sn}^{-1}(\psi, m) \quad \dots(10b)$$

where,  $Sn^{-1}(\psi, m)$  is the function inverse to Jacobi's "sinus amplitudinis", the modulus  $m$  being given by

$$m = \sqrt{\frac{(t_6 - t_5)(t_4 - t_1)}{(t_4 - t_5)(t_6 - t_1)}} = \sqrt{\frac{2(\beta + \sigma)}{(1 + \beta)(1 + \sigma)}} \quad \dots(11)$$

The characteristic co-ordinates for the rectangular field are as follows :

$$\begin{aligned} t=t_4, & & Z=0 \\ t=t_1, & & Z=K \\ t=t_6 = -1, & & Z=iK' \\ t=t_5 = +1, & & Z=K+iK' \end{aligned}$$

where,  $K$  is the complete elliptic integral of the first kind and  $K'$  is the complete complementary elliptic integral of first kind with modulus

$$m' = \sqrt{1 - m^2}$$

#### PRESSURE DISTRIBUTION

The pressure distribution is given by

$$\phi = 100 \left( 1 - \frac{Z}{K} \right) \quad \dots(12)$$

Hence the pressure distribution under the apron is given by

$$\phi_x = 100 \left\{ 1 - \frac{1}{K} Sn^{-1} \left( \sqrt{\frac{(1 + \sigma)(\beta - t)}{(\beta + \sigma)(1 - t)}}, m \right) \right\} \quad \dots(13)$$

in which  $t$  is given by Equation (6) and can be determined for any value of  $\frac{x}{\sqrt{n \cdot D}}$  and  $p$ , from Table I or Figure 17.

For the 'key point'  $E$  (Figure 3),  $t = t_3 = \sigma$

$$\text{ence } \phi_E = 100 \left\{ 1 - \frac{1}{K} Sn^{-1} \left( \sqrt{\frac{(1 + \sigma)(\beta - \sigma)}{(\beta + \sigma)(1 - \sigma)}}, m \right) \right\} \quad \dots(14)$$

Similarly, for the sides of the sheet pile :

$$\phi_y = 100 \left\{ 1 - \frac{1}{K} Sn^{-1} \left( \sqrt{\frac{(1 + \sigma)(\beta \pm t)}{(\beta + \sigma)(1 \pm t)}}, m \right) \right\} \quad \dots(15)$$

in which

$$\begin{aligned} t &= \cos d \sqrt{\tanh^2 y + \tan^2 d} \\ &= \cos \frac{\pi}{2} \cdot p \sqrt{\tanh^2 \frac{\pi}{2} \left( \frac{y}{D} \right) + \tan^2 \frac{\pi}{2} \cdot p} \quad \dots(16) \end{aligned}$$

and can be found from Table I or Figure 17. For the point  $D$  (tip of the pile),  $Y=id$  and  $t=0$

$$\phi_D = 100 \left\{ 1 - \frac{1}{K} \operatorname{Sn}^{-1} \left( \sqrt{\frac{(1+\sigma)\beta}{(\beta+\sigma)}}, m \right) \right\} \quad \dots(17)$$

### List of Symbols

- $A$  = Constant of Schwarz-Christoffel transformation
- $B$  = Half base width of apron on isotropic soil
- $b$  = Base width of apron (original field)
- $D$  = Depth of pervious stratum
- $d$  = Depth of cutoff
- $i$  = Complex number ( $\sqrt{-1}$ )
- $K$  = Complete elliptic integral of first kind of modulus  $m$
- $K'$  = Complete elliptic integral of first kind of modulus  $m'$
- $k_x$  = Coefficient of permeability in  $x$ -direction
- $k_y$  = Coefficient of permeability in  $y$ -direction
- $m$  = Modulus
- $n$  = Anisotropy ratio ( $k_x/k_y$ )
- $p$  = Penetration ratio ( $d/D$ )
- $R, R_1, R_2$  = Resistances
- $x, y$  = Co-ordinates of original anisotropic field
- $x_1, y_1$  = Co-ordinates of isotropic field
- $x'$  = Horizontal distance of any point from the upstream end of floor
- $z$  = Complex co-ordinate =  $x+iy$
- $Z$  = Complex co-ordinate =  $X+iY$
- $\phi$  = Uplift pressure, expressed as percentage of the head causing seepage
- $\phi_x$  = Uplift pressure at any point at distance  $x$  from the origin
- $\phi_E$  = Uplift pressure at key point  $E$
- $\phi_D$  = Uplift pressure at key point  $D$
- $\beta, \sigma$  = Variable dimensions in  $t$ -plane

**References**

- BLIGH, W.G. (1910) : "*Practical Designs of Irrigation Works.*" Second Edition.
- CLIBBORN, C. and BERESFORD, J.S. (1902) : "*Experiment on the Passage of Water through Sand.*" Govt. of India, Central Printing Office.
- KHOSLA, A.N., BOSE, N.K. and TAYLOR, E.M. (1936) : "*Design of Weirs on Permeable Foundation.*" Publication No. 12, Central Board of Irrigation and Power, India.
- PAVLOVSKY, N.N. (1922) : "The Theory of Ground Water Beneath Hydrotechnical Structures." Petesburg.
- PAVLOVSKY, N.N. (1933) : "Motion of Water under Dams." *First Conference on Large Dams*, Stockholm.
- PUNMIA, B.C. (1969) : "Study of Seepage below a Horizontal Impervious Apron founded on Anisotropic Pervious Medium of Finite Depth." *M.E. Thesis*, Department of Civil Engineering, University of Jodhpur.
- WEAVER, W. (1932) : "Uplift Pressure on Dams", *Journal of Mathematics and Physics*, M.I.T. Press, Vol. XI, No. 2.
-